

Article

A New Method for Plasticization of Inclusions in Saw-Wire Steel by NaF Addition

Liangjun Chen ^{1,2}, Yong Wan ¹, Jie Li ^{1,*}, Weiqing Chen ³, Yindong Yang ⁴
and Alexander McLean ⁴

¹ School of Metallurgical Engineering, Anhui University of Technology, Ma'anshan 243002, China; ljchen2016@163.com (L.C.); wanyong0729@ahut.edu.cn (Y.W.)

² Anhui Province Key Laboratory of Metallurgical Engineering & Resources Recycling, Ma'anshan 243002, China

³ State Key Laboratory of Advanced Metallurgy, University of Science and Technology Beijing, Beijing 100083, China; chenweiqing@metall.ustb.edu.cn

⁴ Department of Materials Science & Engineering, University of Toronto, Toronto, ON M5S 3E4, Canada; yy9861@yahoo.com (Y.Y.); amclean16@cogeco.ca (A.M.)

* Correspondence: lsqlijie@126.com; Tel.: +86-173-3067-9619

Received: 6 May 2020; Accepted: 25 May 2020; Published: 27 May 2020



Abstract: In this study, a new method is proposed for the plasticization of inclusions by taking advantage of the behavior of alkali metals in lowering the inclusion melting point. A series of experiments with NaF additions to molten steel were carried out using a carbon tube furnace followed by simulated rolling tests using the solidified ingots and characterization of inclusions with the help of automated scanning electron microscopy. Compositional changes of the steel and evolution of gaseous species were evaluated using thermodynamic software FactSage 7.2 (ThermFact Inc., Montreal, QC, Canada). Based on this approach, NaF/steel/inclusion interactions and the effects of NaF addition on the melting point, size and deformability of inclusions were clarified. The modification of MnO-SiO₂ inclusions by NaF also promoted the removal of inclusions and improved the cleanliness of steel. The results show that with the addition of NaF, the melting point of inclusions is greatly reduced, the deformability is improved, and the removal of inclusions is enhanced, all of which indicates a good prospect for industrial application.

Keywords: saw-wire steel; NaF addition; inclusion modification; deformability

1. Introduction

Saw wire is generally used to cut photovoltaic solar silicon wafers. With the rapid development of the photovoltaic industry, high value-added saw-wire steel has attracted the attention of many researchers. In order to ensure the cutting efficiency and reduce the loss of silicon wafer during the process of cutting, it is necessary to draw saw wire into filaments with an extremely fine diameter [1]. During the process of drawing, hard, non-deformable inclusions are very likely to cause stress concentration, becoming a crack initiator, and leading to wire breakage [2,3]. The diameter of ultra-fine saw wire is between 65 and 80 μm , which is much smaller than that of steel cord for automobile tires (150–380 μm). Therefore, more stringent control of inclusions is required in saw-wire steel than in tire cord steel [4]. Thus, the traditional technology of Si-Mn deoxidation combined with low basicity top slag for inclusion control of tire cord steel does not fully meet the strict requirements of saw-wire steel. There are still frequent incidents of wire breakage caused by non-deformable inclusions during the process of drawing or cutting silicon wafers which significantly reduces production efficiency and leads to substantial economic losses. Therefore, there is an incentive to develop a more efficient method for controlling inclusions during the production of saw-wire steel.

Although the deformability of inclusions is related to their hardness, elastic modulus, size, crystal structure, viscosity and melting point, their melting point is considered to be the key factor [5,6]. It is widely accepted that inclusions with low melting point have good deformability. Most of the research on plasticization of inclusions is based on the concept of lowering their melting point [7–19]. Guo et al. found that non-deformable Al_2O_3 inclusions in aluminum killed steel can be modified into $\text{Al}_2\text{O}_3\text{-CaO-MgO-CaS}$ inclusions with a lower melting point and better deformability by calcium treatment [7]. Qin et al. noted that the increase of MgO content enlarges the liquid area of the $\text{CaO-SiO}_2\text{-Al}_2\text{O}_3\text{-MgO}$ system based on the phase diagram obtained from FactSage calculations. This means that MgO has the potential to lower the melting point and therefore improve the deformability of inclusions. By treating 82B high carbon steel with magnesium they observed that the deformability of inclusions was enhanced and the tensile strength of wire rods was increased by about 17% [8]. Li et al. pointed out that hard and non-deformable Al_2O_3 inclusions in steel can be modified into deformable rare earth aluminate inclusions by adding proper amount of rare earth elements [9]. Cui et al. proposed a new method of inclusion plasticization in Si-Mn killed tire cord steel by adding B_2O_3 . According to FactSage calculations the melting points of $\text{CaO-SiO}_2\text{-Al}_2\text{O}_3$ and $\text{MnO-SiO}_2\text{-Al}_2\text{O}_3$ inclusions decrease significantly with the addition of 5% and 10% B_2O_3 , respectively. This method successfully enhanced the deformability of inclusions in tire cord steel [10]. Wang et al. pointed out that alkali metal oxides are effective in lowering the melting point of oxide melts [11]. Based on this observation, Sakamoto et al. obtained plasticization of inclusions in high carbon steel with the addition of a range of compounds containing alkali metals, which greatly lowered the melting point of inclusions [12]. Inclusions containing lithium have been generated in tire cord steel by feeding Li alloy wire, Li alloy or injecting Li powder with an inert carrier gas. These inclusions have better deformability and smaller size, which produced a lower rate of wire breakage during laboratory drawing tests [13]. The authors of the present study put forward a new method of adding alkali metal into saw-wire steel by mixing iron powder with alkali carbonates for the purpose of inhibiting the violent volatilization of carbonate and thus obtaining a high yield. By this method, the melting point of inclusions was notably lowered, and their deformability was significantly improved [14]. While the research described above has made some progress in achieving the plasticization of inclusions, the industrial application of the findings has not been realized due to practical difficulties, such as metal sputtering caused by high volatility of additives and unsatisfactory plasticization. Among studies on plasticization, refining technologies with low basicity top slag have attracted the most attention and become the plasticization technology that has achieved large-scale industrial application [15–19]. This technology is mainly employed for tire cord steel. Through steel/slag/inclusion interactions, inclusion composition is precisely controlled within a low melting regime which promotes the plasticization of inclusions. This technology has been widely used due to the advantages of low cost and high stability. Nonetheless, the extent of reduction in the melting point of inclusions by this technology is limited, and while it can meet the requirements for tire cord steel, the quality requirements of saw-wire steel are more stringent. In view of the excellent performance of alkali metal on lowering the melting point of inclusions, the addition of alkali is expected to meet the strict requirements of saw-wire steel for the deformability of inclusions. However, most of the previous technologies of alkali metal addition use alkali metal carbonate as an additive, which has a low boiling point and is easy to decompose. This causes a series of problems, such as violent splashing of molten steel, low yield and major composition fluctuation, all of which limit the industrial application of alkali metal addition. To solve these problems, it is necessary to explore a more efficient and stable alkali metal addition method in order to promote the industrial application of this technology for inclusion plasticization.

In view of the high boiling point 1968 K and the good stability of NaF, a new method is proposed for alkali metal addition using NaF rather than unstable alkali metal carbonate, aimed at inclusion control in saw-wire steel. In this study, the reaction between steel and NaF is simulated using FactSage software, the rolling process is simulated by air forging hammer, and inclusions are analyzed by automated scanning electron microscopy equipped with the software INCA FEATURE

(OXFORD INSTRUMENTS Ltd, Abingdon, Oxfordshire, UK). Based on this study, a mechanism for the transfer of Na from NaF to inclusions is proposed, the evolution of inclusions after NaF addition is described, and the effects of NaF addition on inclusion melting point and deformability were established. These findings provide a scientific basis for the implementation of a new technology for inclusion plasticization.

2. Experimental Aspects

2.1. Material Preparation

A piece of continuous cast slab taken from the production process of Si–Mn-killed saw-wire steel was cut into small blocks and prepared as initial charge steel material. These blocks were then cleaned with hydrochloric acid to remove the oxide layer on the surface, washed with alcohol and oven-dried. In order to avoid possible interference from slag during inclusion analysis, no slag was used in the experiments. NaF (AR, 99.9%, Sinopharm Chemical Reagent Co, Ltd, Shanghai, China) powder was mixed with the same amount of iron powder (AR, 99.9%, Sinopharm Chemical Reagent Co, Ltd, Shanghai, China) to inhibit the volatilization of NaF, pressed into compacts and wrapped with thin pure iron sheets. These compacts were attached to the end of a pure iron rod for easy addition to the melt, thus simulating the feeding process in actual production.

2.2. Experimental Equipment

The melting experiments were performed in a resistance furnace with a graphite tube heating element, as shown in Figure 1. An Al_2O_3 tube was used as a reaction chamber to avoid carbon pick-up caused by the graphite tube. Throughout each experiment, argon gas was injected into the bottom of the reaction chamber to avoid the oxidation of molten steel. Before the experiments, a B-type (Pt-30% Rh/Pt) thermocouple was used to calibrate the internal thermocouple that indicated the furnace temperature within ± 5 K.

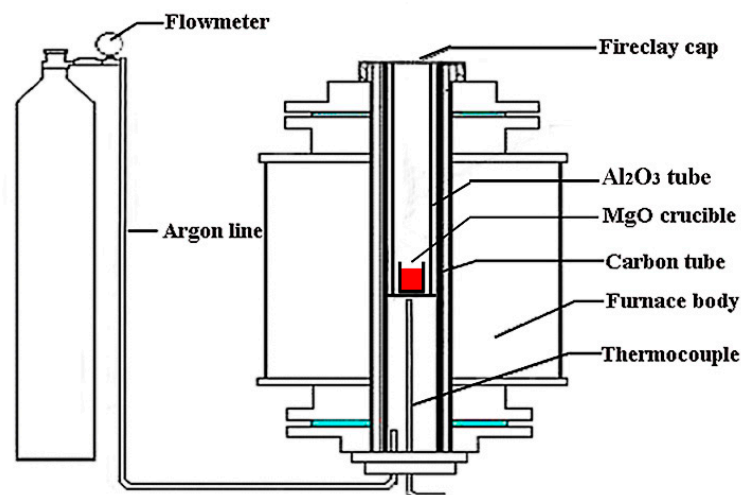


Figure 1. Schematic diagram of the graphite tube resistance furnace.

2.3. Experimental Procedure

Four heats were carried out with different amounts of additions as shown in Table 1. First, 300 g of the initial steel material was placed in a MgO crucible and heated to 1823 K in the graphite tube resistance furnace. The prepared compact of NaF and iron powder was inserted into the molten steel. For Heats A to C, after holding at 1823 K for 15 min, the molten steel contained in the MgO crucible was quickly water quenched. In order to investigate the deformability of the inclusions, the cooled ingots were heated in a muffle furnace at 1373 K for 1 h and then forged into wire rods with a diameter

of 7 mm, thus simulating the rolling process in actual production. Steel samples were taken from the wire rods and prepared as metallographic samples in the longitudinal direction by using a resin mount, grinding, polishing and gold-spraying. To study the evolution process of inclusions after NaF addition, one more heat was carried out and this is denoted as Heat D. For Heat D, the temperature was held constant at 1823 K for 45 min. During this period, samples were withdrawn from the melt using a quartz tube coupled with a rubber suction bulb and rapidly quenched in water at various times after addition of the NaF compact: 0 min, 15 min, 30 min and 45 min. The steel samples were then prepared for metallographic examination as described previously.

Table 1. Composition of additives.

Heats No.	NaF Amount/g	Fe Amount/g
A	0.5	0.5
B	1	1
C	2	2
D	1.5	1.5

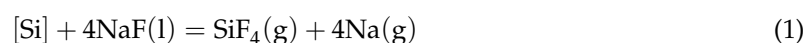
2.4. Analysis

For the initial steel material and Heats A, B and C, [C], [Si] and [Mn] were determined by optical emission spectrometry (OES), while the key element [Na] was evaluated by inductively coupled plasma mass spectrometry (ICP-MS) for higher accuracy. Total oxygen content (T.O.) was measured with the infrared X-ray absorption method. Inclusions in the steel samples were evaluated both automatically and manually. A scanning electron microscope equipped with energy dispersive spectrometry (EDS) and software for automated inclusion analysis was employed to evaluate the inclusions. Inclusion morphology information, including size, number and aspect ratio was gathered automatically from an area of 22.9 mm² on the polished surface of the metallographic samples. The size of the inclusions was calculated based on the equivalent circle diameter (ECD). In view of possible inaccuracy using the automatic scan with a short EDS analysis time of 0.2 s, 30 inclusions in each sample were also evaluated by manual EDS analysis for a period of 30 s.

3. Results and Discussion

3.1. Effects of NaF Addition

The compositions of the initial steel material and also the steel after reaction are shown in Tables 2 and 3, respectively. It can be seen that the contents of [C], [Si] and [Mn] decreased compared with the composition of the initial material. This is due to air entering the reaction chamber and oxidizing the molten steel during the addition of NaF. In addition, the actual trace amount of [Na] in the steel was not determined since it was below the lower limit of detection by ICP-MS analysis. For these reasons, it is difficult to infer the reaction mechanism between NaF and molten steel based on the change of steel composition. In order to clarify the transfer mechanism of Na from NaF to the molten steel, the equilibrium reaction between molten steel and NaF was simulated using the Equilib module of FactSage 7.2, selecting the databases of FactPS, FToxid and FSstel. The calculated reaction temperature was selected as 1823 K and the initial composition of steel was set as 0.87C, 0.17Si, 0.52Mn, 0.0007Al, 0.001O (wt%). The results of the simulation are shown in Figure 2 from which it can be seen that with the increase of NaF amount, the contents of [C] and [Mn] in steel remained almost unchanged while the [Si] content decreased gradually (Figure 2). This was accompanied with the generation of Na (g) and SiF₄ (g) while at the same time some NaF (g) evaporated (Figure 2b). This implies that the reaction between NaF and steel can be represented as shown in Equation (1):



During the addition of NaF there was no violent fluctuation or splashing observed at the surface of the molten steel. This suggests that NaF did not volatilize or decompose violently, which meets the requirements of stability and safety for NaF addition in industrial production. Nevertheless, a small amount of white fume was generated at the initial stage of NaF addition. The fume condensed into white powder on the cover of the furnace and was collected for X-ray diffraction analysis. As shown in Figure 3, the collected powder was mainly composed of NaF and Na, which implies the generation of NaF (g) and Na (g). SiF₄ (g) has a low boiling point and did not condense on the cover of the furnace, which explains the absence of SiF₄ in the collected powder. These experimental results are consistent with the calculated values, which confirms the existence of Reaction (1). Inevitably, part of the generated Na (g) will dissolve in the molten steel and react with inclusions. The dissolution process is expressed as Equation (2). Equation (1) can be combined with Equation (2) to provide Equation (3) which indicates the transfer mechanism of Na from NaF to molten steel. During the experiment, some NaF and SiF₄ fume escaped from the molten steel due to a lack of protection from slag. In actual production however, the surface of molten steel is covered with a thick slag layer that absorbs toxic fume and reduces environmental pollution.

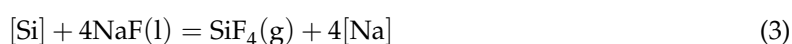


Table 2. Composition of initial steel (wt%).

[C]	[Si]	[Mn]	[Al]	[Ca]	[Mg]	[Na]	T.O.
0.87	0.17	0.52	0.007	<0.0003	0.0002	<0.005	0.001

Table 3. Composition of steel after reaction (wt%).

Heats No.	[C]	[Si]	[Mn]	[Na]
A	0.86	0.15	0.50	<0.005
B	0.84	0.14	0.51	<0.005
C	0.82	0.12	0.51	<0.005

Na-containing inclusions were detected in all heats and their typical morphology and energy spectrum results are shown in Figure 4. This confirms that Na within NaF had successfully transferred into inclusions. The typical morphologies and compositions of inclusions in wire rods from Heats A, B and C are shown in Figure 5. It can be seen that the inclusions can be grouped into two categories: Na-containing inclusions and Na-free MnO-SiO₂ inclusions. Compared with the MnO-SiO₂ inclusions, the Na-containing inclusions have lower contents of SiO₂ and MnO. Compared with blocky Na-free (non-modified) MnO-SiO₂ inclusions, the Na-containing (modified) inclusions were elongated string-like shapes in the rolling direction. This confirms that it is feasible to achieve inclusion plasticization by adding NaF into saw-wire steel.

The average MgO and Al₂O₃ contents of the 90 inclusions measured manually in wire rods from Heats A, B and C are 5% and 8%, respectively. In order to show the changes in inclusions from Heat A to Heat C on the same phase diagram, the inclusions are plotted on the diagram shown in Figure 6 which represents the system Na₂O-SiO₂-MnO- (5%)MgO- (8%)Al₂O₃ with an 1373 K isotherm, defined as a low melting point regime. It can be seen that with the increase of NaF addition from 0.5 g (Heat A) to 2 g (Heat C), inclusions gradually moved towards the direction of higher Na₂O, lower MnO and lower SiO₂ contents. Accordingly, the proportion of inclusions with a melting point lower than 1373 K increased from 50% to 86.7%.

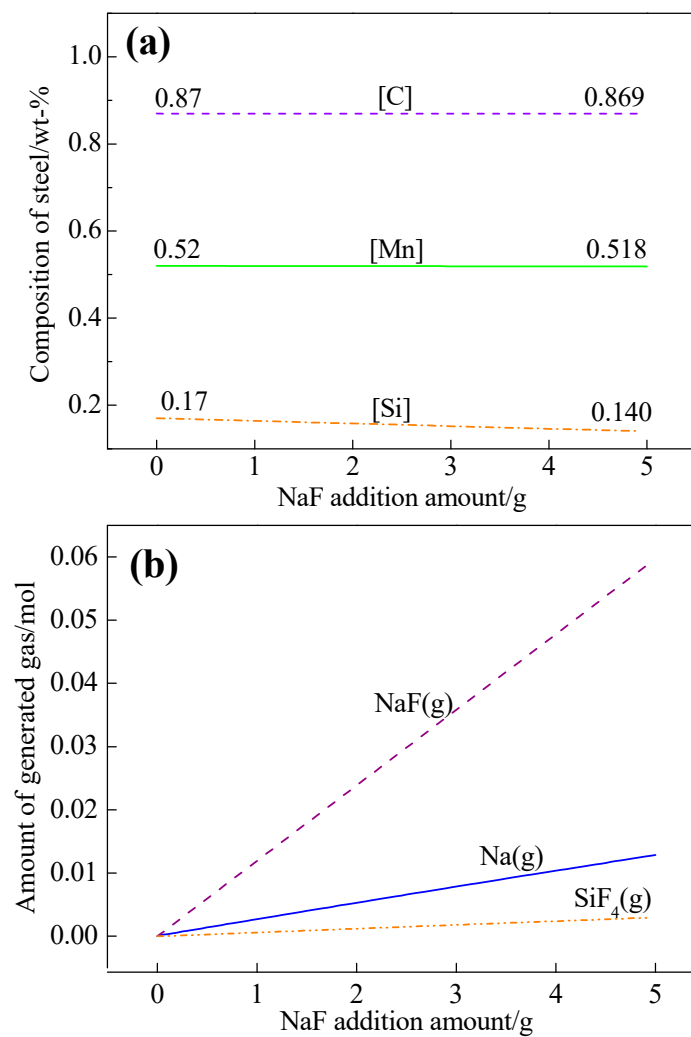


Figure 2. Gas generation after NaF addition in liquid steel at 1823 K. Calculated results using FactSage 7.2. (a) Composition change of steel with NaF addition; (b) amount of generated gas with NaF addition.

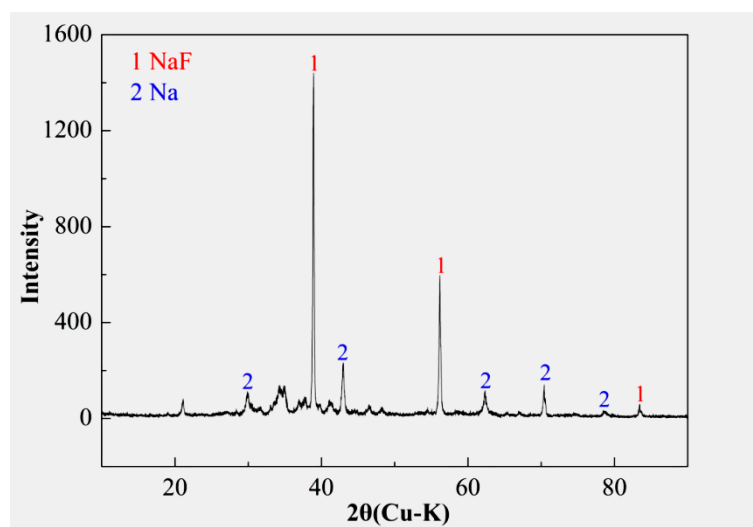


Figure 3. XRD result of the white powder collected from the cover of the furnace.

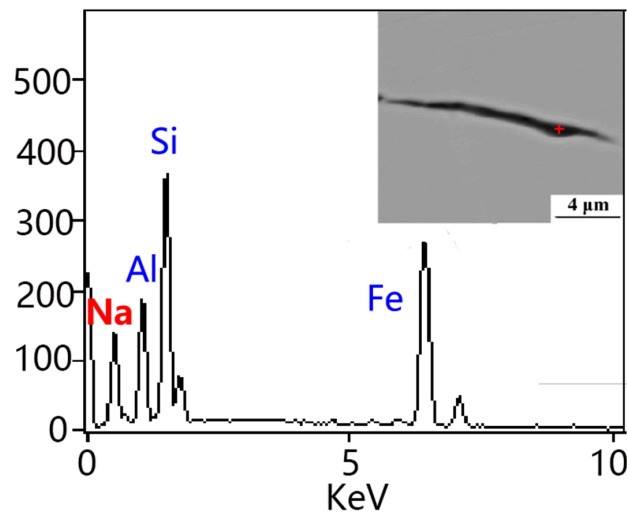


Figure 4. Typical morphology and energy spectrum of Na-containing inclusions.

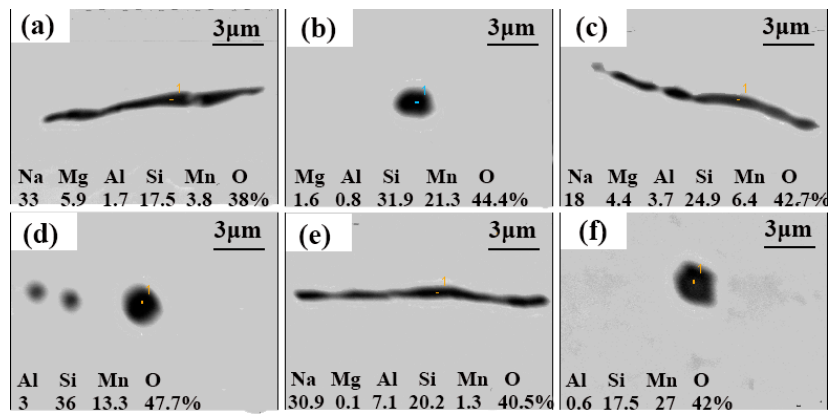


Figure 5. Typical morphologies and compositions of inclusions in wire rods from Heats A, B and C (wt%). (a,b) represent Heat A; (c,d) represent Heat B; (e,f) represent Heat C.

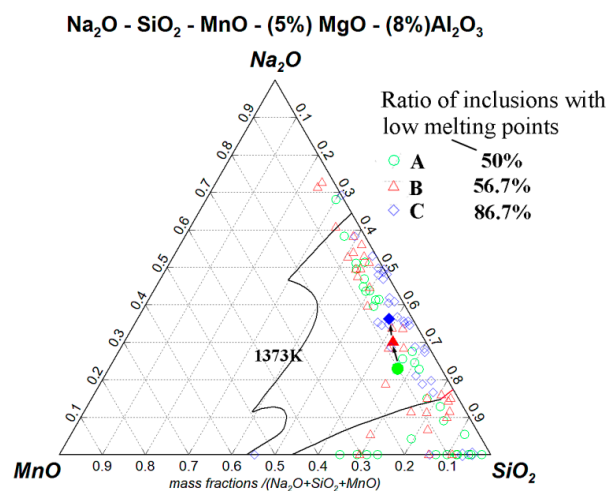


Figure 6. Distribution of inclusions in wire rods from Heats A, B and C. Solid symbols represent the average composition in each heat.

Inclusions with an aspect ratio more than 3 are defined as plastic inclusions, and the ratio of plastic inclusions can be regarded as an indicator to measure the effect of NaF addition on plasticization.

The proportion of inclusions with a low melting point obtained from Figure 6 and the proportion of plastic inclusions collected by automatic SEM evaluation are shown in Figure 7. It is clear that there is a correlation between the proportions of low melting point inclusions and plastic inclusions, which is consistent with the general view that inclusions with low melting point have good deformability. With the increase of NaF addition from Heat A to Heat C, the proportion of plastic inclusions increased gradually from 28.5% to 51.6%, accordingly the plasticization effect of inclusions by NaF was enhanced.

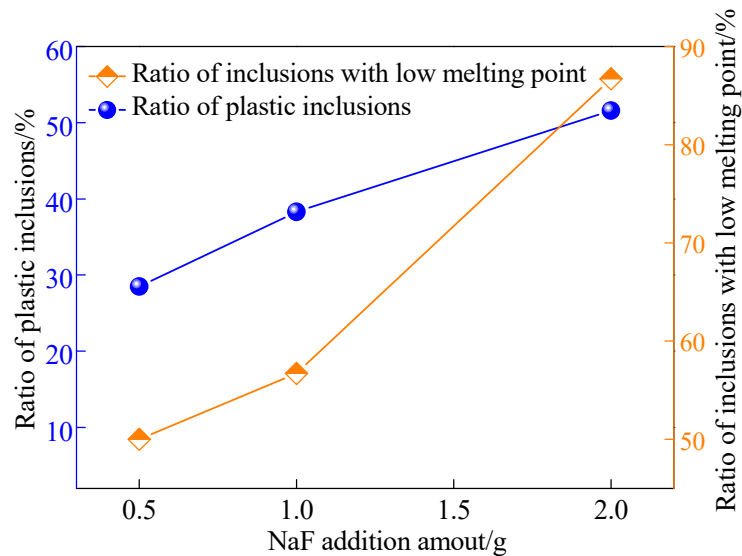


Figure 7. Relationship of the melting performance and deformability of inclusions with NaF addition.

The decrease in inclusions with NaF addition is shown in Figure 8. With the increase of NaF, the quantity of Na-containing inclusions increased while the quantity of MnO-SiO₂ inclusions decreased significantly. This was attributed to the modification of MnO-SiO₂ inclusions into Na-containing inclusions and their more rapid flotation due to their larger size. It can be concluded from Figure 8 that NaF addition promoted the removal of inclusions and improved the cleanliness of saw-wire steel.

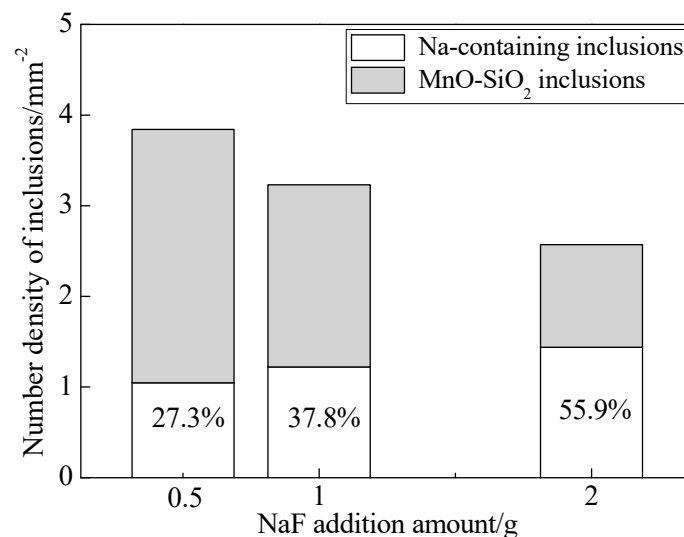


Figure 8. Relationship between inclusion quantity and NaF addition.

The composition of inclusions in Heats A, B and C measured with manual EDS analysis fall into a regular change pattern with increasing Na₂O, as shown in Figure 9. Na₂O in inclusions is a characteristic composition introduced by the interaction between inclusions and molten steel, thus the

Na₂O content can be regarded as an indicator of the interaction extent between molten steel and inclusions. It can be seen that with the increase of Na₂O content among inclusions (i.e., the increase of reaction extent between molten steel and inclusions), the corresponding MnO and SiO₂ contents gradually decrease. That is to say, as the interaction progresses, [Na] in molten steel replaced Mn and Si within oxides in inclusions. It thus can be deduced that [Na] in steel enters into inclusions by reduction reaction as expressed by Equations (4) and (5) below. In addition, it can be seen that MnO preferentially decreased to a relatively low level before SiO₂ content began to decrease. This implies that Equation (4) took place prior to Equation (5).

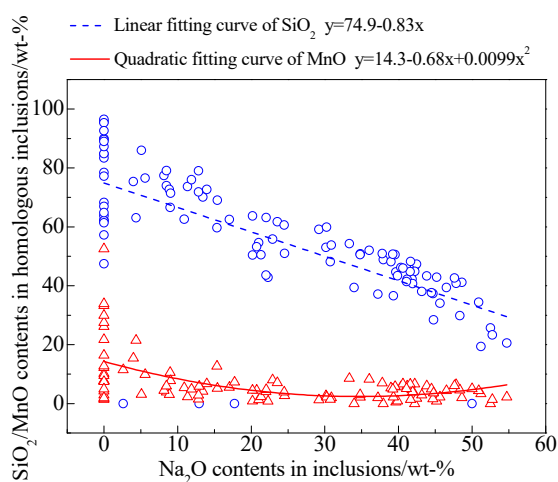
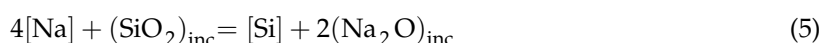
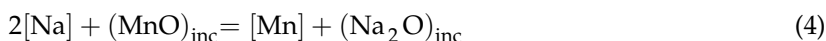


Figure 9. Compositional changes with Na₂O content in inclusions from Heats A to C.

3.2. Mechanism of Inclusion Modification

Based on the above analysis, a potential mechanism for inclusion modification by NaF addition can be proposed, as shown schematically in Figure 10. After addition to the steel of NaF, the powder transforms into liquid droplets. Part of the NaF volatilizes to produce NaF (g), part is reduced to Na (g) and SiF₄ (g) by [Si] in the steel, and part of the generated Na (g) dissolves into the molten steel. This transformation process can be expressed by Equation (3). Part of the generated Na (g) and NaF (g) escape from the molten steel, as evidenced by the existence of these species on the furnace cover. Because of the strong affinity of Na for oxygen, the [Na] in steel reduces the MnO and SiO₂ in the inclusions, as expressed by Equations (4) and (5). This process of Na migration from steel to inclusions is confirmed by the fact that the contents of MnO and SiO₂ gradually decrease with increasing Na₂O content in the inclusions as shown in Figure 9.

3.3. Evolution of Inclusions

As shown in Figure 11, Na-containing inclusions and MnO-SiO₂ were the only types of inclusions detected during the process of sampling Heat D. Both types of inclusions are spherical, indicating that they are liquid at the experimental temperature (1823 K). Compared with the MnO-SiO₂ inclusions, the Na-containing inclusions have lower contents of MnO and SiO₂ and are a larger size.

In order to compare the size of the two types of inclusions more accurately, inclusions in Heat D were counted by automated software, grouped by inclusion type and plotted in Figure 12. It is clear that Na-containing inclusions have a larger size than MnO-SiO₂ inclusions. According to the Navier–Stokes equation [20], Na-containing inclusions with larger size are more likely to be removed by flotation than unmodified MnO-SiO₂ inclusions. This suggests that inclusion modification by NaF

promotes the removal of inclusions and improves cleanliness, which is in accord with the findings shown in Figure 8.

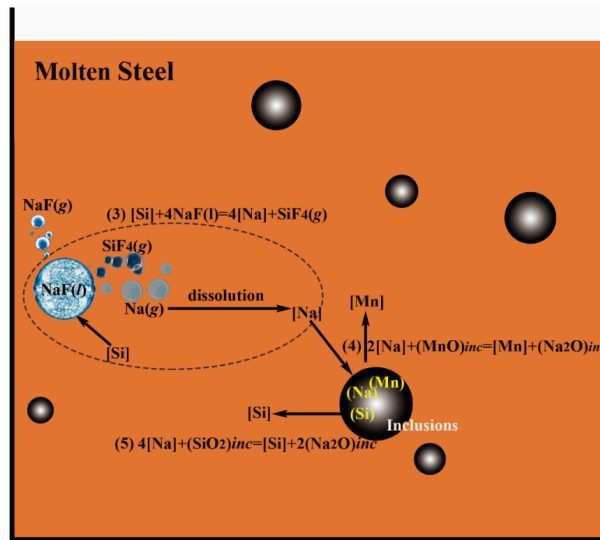


Figure 10. Schematic diagram of inclusion modification by NaF treatment.

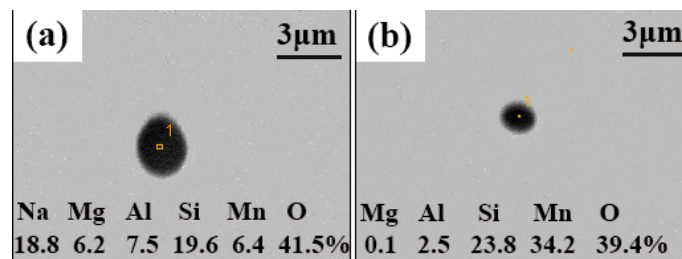


Figure 11. Typical morphologies and composition (wt%) of inclusions in Heat D (a) represents the typical Na-containing inclusion, (b) represents the typical MnO-SiO₂ inclusion.

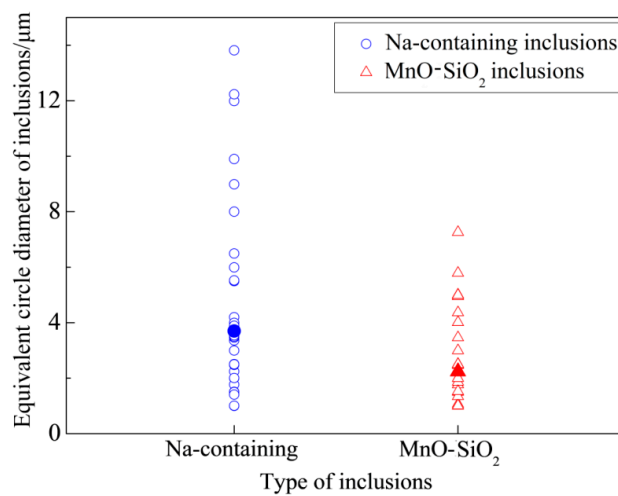


Figure 12. Relationship between size and type of inclusions (the filled symbols denote the average size of a certain type of inclusion).

In order to clarify the evolution of inclusions in Heat D after NaF addition, the quantity of both kinds of inclusions after various times was determined by automated software and the results are

shown in Figure 13. It can be seen that a large number of Na-containing inclusions appear in the steel immediately (0 min) after adding NaF. This suggests that inclusion modification by NaF can be completed in a very short time at high temperature. As time progressed after NaF addition, the quantity of MnO-SiO₂ inclusions changes little while the quantity of Na-containing inclusions clearly decreased. This confirms the previous conclusion that Na-containing inclusions are more likely to be removed by flotation than MnO-SiO₂ inclusions. Thus, by transforming MnO-SiO₂ inclusions into Na-containing inclusions, the addition of NaF facilitates inclusion removal and improves the cleanliness of the steel.

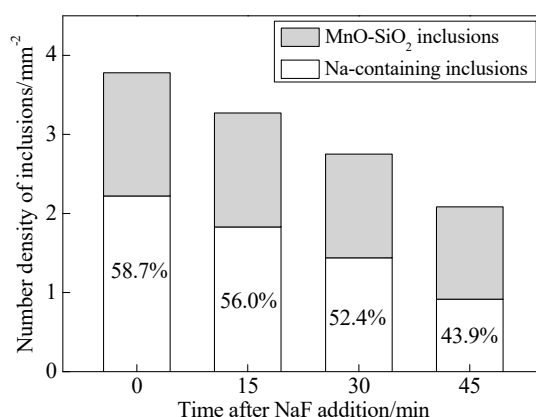


Figure 13. Quantity of inclusions at different times after NaF addition in Heat D.

The composition of inclusions in Heat D was plotted on the phase diagram shown in Figure 14 by a method similar to that used to plot Figure 6. It can be seen that the distribution of inclusions moves toward a direction of lower Na₂O, but higher MnO and SiO₂ as time progressed after NaF addition due to the removal of a large amount of Na-containing inclusions as shown in Figure 13. Most of the inclusions at various stages after NaF addition are distributed within the low melting regime, which confirms the good effect of NaF on lowering the melting point of inclusions.

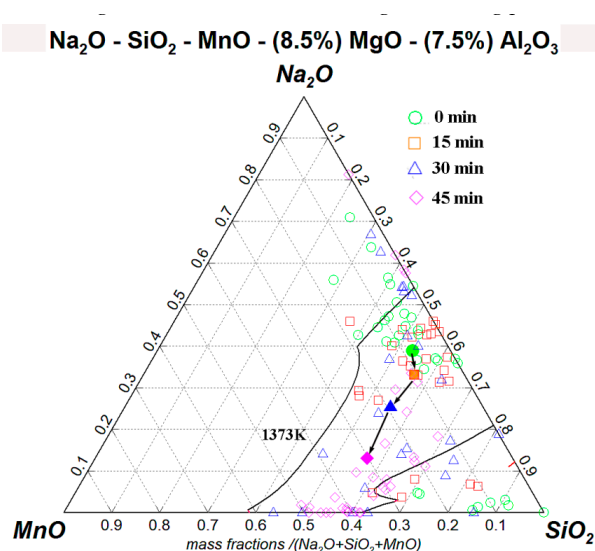


Figure 14. Distribution of inclusions at different times after NaF addition in Heat D (the solid symbols represent the average composition at different times).

The composition of inclusions in samples from Heat D as determined by manual EDS analysis shows that the corresponding MnO and SiO₂ contents gradually decrease with the increase in Na₂O

content of the inclusions, as shown in Figure 15. This is similar to the observations reported in Figure 9 and provides further confirmation of the validity of Equations (4) and (5).

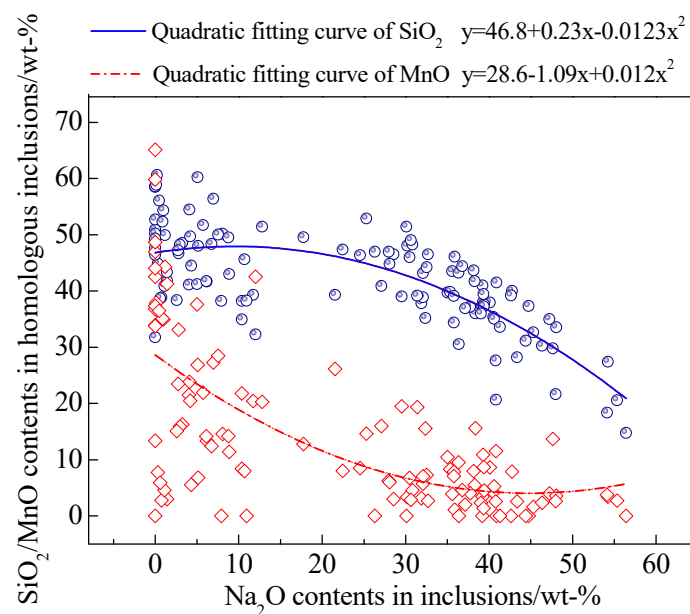


Figure 15. Compositional changes with Na_2O content in inclusions from Heat D.

4. Conclusions

To meet the urgent requirement of saw-wire steel for improvement of inclusion plasticization and thus prevent wire breakage, a new method of plasticization by NaF addition is proposed. The work is aimed at solving the problems of violent splashing, low yield and wild fluctuation during the process of plasticization by adding NaF into the molten steel rather than alkali metal carbonates. The transfer mechanism of Na involving NaF/steel/inclusion interactions, the evolution of inclusions with time after NaF addition and the effects of different NaF addition amounts, were all investigated. The conclusions can be summarized as follows:

- (1) The Na-containing inclusions were generally larger than the MnO-SiO₂ inclusions and were therefore more likely to be removed by flotation. Thus, NaF addition promoted inclusion removal and improved cleanliness of the steel by modifying MnO-SiO₂ inclusions into Na-containing inclusions;
- (2) With the increase of NaF addition, the proportion of Na-containing inclusions with low melting point increased and the proportion of plastic inclusions showed a relevant increasing tendency.
- (3) The modification mechanism of inclusions by NaF is generalized as two steps:

Step 1: Silicon in the molten steel reacts with NaF droplets through Reaction $[\text{Si}] + 4\text{NaF} (\text{l}) = \text{SiF}_4 (\text{g}) + 4[\text{Na}]$ to generate $[\text{Na}]$ in steel.

Step 2: The generated $[\text{Na}]$ then transferred into inclusions by reducing the MnO or SiO₂ in inclusions through Reaction $2[\text{Na}] + (\text{MnO})_{\text{inc}} = [\text{Mn}] + (\text{Na}_2\text{O})_{\text{inc}}$ and $4[\text{Na}] + (\text{SiO}_2)_{\text{inc}} = [\text{Si}] + 2(\text{Na}_2\text{O})_{\text{inc}}$, thus modifying the inclusions.

Author Contributions: Conceptualization, L.C. and W.C.; methodology, L.C. and J.L.; software, L.C. and Y.W.; validation, J.L., Y.Y. and A.M.; formal analysis, Y.Y. and A.M.; investigation, J.L.; resources, W.C.; data curation, J.L. and Y.W.; writing—original draft preparation, L.C. and J.L.; writing—review and editing, W.C., Y.Y. and A.M.; visualization, L.C. and Y.W.; supervision, W.C. and J.L.; project administration, W.C. All authors have read and agreed to the published version of the manuscript.

Funding: This research received no external funding.

Conflicts of Interest: The authors declare no conflict of interest.

References

1. Kiriwara, K. Production technology of wire rod for high tensile strength steel cord. *Kobelco Technol. Rev.* **2011**, *30*, 62–65.
2. Son, S.; Lee, Y.K.; Kang, S.H.; Chung, H.; Cho, J.S.; Moon, J.; Oh, K.H. A numerical approach on the inclusion effects in ultrafine gold wire drawing process. *Eng. Fail. Anal.* **2011**, *18*, 1272–1278. [[CrossRef](#)]
3. Norasethasophon, S.; Yoshida, K. Prediction of chevron crack initiation in inclusion copper shaped-wire drawing. *Eng. Fail. Anal.* **2008**, *15*, 378–393. [[CrossRef](#)]
4. Chen, C.; Jiang, Z.; Li, Y.; Sun, M.Y.; Chen, K.; Wang, Q.; Li, H. Effect of Na₂O and Rb₂O on inclusion removal in C96 V saw-wire steels using low-basicity LF (Ladle Furnace) refining slags. *Metals* **2018**, *8*, 691. [[CrossRef](#)]
5. Bertrand, C.; Molinero, J.; Landa, S.; Elvira, R.; Wild, M.; Barthold, G.; Valentin, P.; Schifferl, H. Metallurgy of plastic inclusions to improve fatigue life of engineering steels. *Ironmak. Steelmak.* **2003**, *30*, 165–169. [[CrossRef](#)]
6. Guo, J.; Chen, S.S.; Chen, Z.J. Mechanism of non-metallic inclusion formation and modification and their deformation during compact strip production (CSP) process for aluminum-killed steel. *ISIJ Int.* **2013**, *53*, 2142–2151.
7. Kanaun, S.; Martinez, R. Numerical solution of the integral equations of elasto-plasticity for a homogeneous medium with several heterogeneous inclusions. *Comput. Mater. Sci.* **2012**, *55*, 147–156. [[CrossRef](#)]
8. Qin, J.S.; Qu, T.P.; Wang, D.Y.; Hu, M.; Tian, J. Mg treatment process for high carbon steel 82B. *Steelmaking* **2019**, *35*, 18–23.
9. Li, C.R.; Yang, H.; Wen, H. Thermodynamic analysis of modification treatment of rare earth elements on inclusions in hard wire steel. *Hot Work. Technol.* **2010**, *39*, 12–14.
10. Cui, H.Z.; Chen, W.Q. Effect of boron on morphology of inclusions in tire cord steel. *J. Iron Steel Res. Int.* **2012**, *19*, 22–27. [[CrossRef](#)]
11. Wang, W.; Sun, K.; Liu, H. Effects of different aluminum sources on morphologies and properties of ceramic floor tiles from red mud. *Constr. Build. Mater.* **2020**, *241*, 118119. [[CrossRef](#)]
12. Sakamoto, K.; Sugimura, N.; Yoshida, N. A Method of Producing High-Purity Steel with High Fatigue Strength and High Cold Processing. China Patent Application No. CN1836052A, 20 September 2006.
13. Sakamoto, K.; Sugimura, T.; Yoshida, A.; Fukuzaki, Y.; Suda, S. Method for Producing High Cleaness Steel Excellent in Fatigue Strength or Cold Workability. U.S. Patent Application No. 7,608,130 B2, 27 October 2009.
14. Chen, L.; Chen, W.J.; Hu, Y.; Chen, Z.; Xu, Y.; Yan, W. Effect of Na₂CO₃ addition on inclusions in high-carbon steel for saw wire. *Trans. Indian Inst. Met.* **2018**, *71*, 383–391. [[CrossRef](#)]
15. Kang, Y.B.; Jung, I.H.; Deckerov, S.A.; Pelton, A.D.; Lee, H.G. Critical thermodynamic evaluation and optimization of the CaO-MnO-SiO₂ and CaO-MnO-Al₂O₃ systems. *ISIJ Int.* **2004**, *44*, 965–974. [[CrossRef](#)]
16. Tomioka, K.; Ogawa, K.; Matsumoto, H. Thermodynamics of reaction between trace amount of Al and inclusion in Mn-Si killed steel. *ISIJ Int.* **1996**, *36*, S101–S104. [[CrossRef](#)]
17. Choudhary, S.K.; Chandra, S.; Ghosh, A. Prediction of deoxidation and inclusion precipitation in semi-killed steel. *Metall. Mater. Trans. B* **2005**, *36*, 59–66. [[CrossRef](#)]
18. Bernard, G.; Ribound, P.V.; Urbain, G. Oxide inclusions plasticity. *Rev. Metallurgie-CTT* **1981**, *78*, 421–433. [[CrossRef](#)]
19. Mandal, G.K.; Kamaraj, A.; Humane, M.M.; Minj, R.K.; Das, S.K.; Ramana, R.V.; Venugopalan, T. Development of specialty grade wire by controlling the inclusions in high-carbon steel using synthetic slag treatment. *Trans. Indian Inst. Met.* **2019**, *72*, 369–381. [[CrossRef](#)]
20. Jha, P.K.; Rao, P.S.; Dewan, A. Effect of height and position of dams on inclusion removal in a six strand tundish. *ISIJ Int.* **2008**, *48*, 154–160. [[CrossRef](#)]

